E-ISSN: 2581-3463

AJMS
Asian Journal of Mathematical Sciences

RESEARCH ARTICLE

NUMERICAL ANALYSIS OF ETHYLENE GLYCOL BASED HYBRID NANOFLUID AS A COOLANT FOR AUTOMOTIVE RADIATORS

*** Sospeter Wabwile Wanyonyi, Winfred Nduku Mutuku[1]**

* *Department of Mathematics, Kenyatta University*

[1]*Department of Mathematics,Kenyatta University, P.O. Box 43844-00100, Nairobi,Kenya.*

Corresponding Email: wabwile.sospeter@gmail.com

Received: 10-4-2026; Revised: 20-05-2026; Accepted: 15-06-2026

ABSTRACT

In this paper, the cooling potential of hybrid nanofluid containing ethylene glycol with three types of nanoparticles: Cu- Al_2O_3, Cu- ZnO and CuO- ZnO is investigated for their suitability as industrial coolants. Nanofluids are obtained by dispersing micron-sized nanoparticles in a base fluid. They possess better thermophysical properties compared to convection fluids. Advancement in technology has created the need to develop shrunk devices though with intensified processes to achieve aesthetics. As a result, ordinary fluids and nanofluids are however becoming unsuitable due to their incapacity to fully eliminate heat from the modern engines. This therefore calls for coolants exhibiting higher thermal properties. Hybrid nanofluids, obtained by dispersing two types of nanoparticles in a base fluid, are highly recommended as a remedy. They withstand the excess heat liberated which may cause wear and tear of engine parts. They are utilized as industrial heat transfer fluids in automotive, geothermal, solar energy, electronics, and biomedical fields due to their enhanced thermal physical properties. The governing equations were formulated from the general equations governing the fluid flow. The resultant equations were non-dimensionalised and then solved using the fourth order Runge Kutta method. The results are presented graphically and discussed putting into consideration their industrial applications. The study emphasized the effects of pertinent parameters on fluid velocity, temperature, skin friction, and rate of heat transfer. The results revealed that Aluminium oxide- Zinc Oxide/EG- water hybrid nanofluid exhibited higher rate of heat transfer and lower skin friction compared to Cu-H_2O nanofluid, highlighting its great potential for enhanced thermal management in automotive radiators.

Keywords: Hybrid Nanofluid; Coolant; Radiator; Convective heating,

INTRODUCTION

Modern electronic and automotive industries have increased demand for cooling systems with smaller surface areas but exhibiting high thermal performance. This calls for an optimization procedure with an optimal design that balances functionality, portability, and aesthetics as a remedy. Researchers have tried a number of different approaches, performing tests using ethylene glycol and water distributed in different ways to learn more about heat transfer properties for automotive radiators.

Choi [1] in their research discovered that dispersing particles smaller than micron-sized particles in a base fluid would significantly increase its thermal conductivity. The resultant fluid they identified it as a nanofluid. They noted that dispersing more nanoparticles in the base fluid or rather increasing the temperatures of the nanofluids at even lower nanoparticle composition increases the thermal conductivity of the nanofluids. Golden [2] in addition included the condition that the particles must be in colloidal suspension. Nanofluids, due to the complicated interplay of the electrical conductivity of nanoparticles with that of the base fluid, are more vulnerable to the effects of a magnetic field than conventional base fluid as stated by Mutuku and Makinde [3]. Hussein [4] studied two nanofluids comparing their local Nusselt number, friction factor and effectiveness. Results showed that the Nusselt number greatly depended on volume fraction and the Reynolds number. $SiO2$ depicted higher local Nusselt number than $TiO2$ nanofluid.

In a study by Dhaiban [5] using ZnO - ethylene glycol based nanofluids with a critical look at its thermal physical properties noticed an improvement in thermal conductivity of 26.5% having added a 5% volume fraction of ZnO nanoparticles in ethylene glycol as the base fluid. Similar results were revealed on using $Al2O3$/water nanofluids following an increase in nanoparticle concentration.

We can thus deduce from the above observations that use of single phase nanofluids in a base fluid greatly enhances thermal conductivity of nanofluids. Moreover, dispersion of two or more nanoparticles in a base fluid exhibits better thermal conductivity compared to use of convective fluids as well as single phase nanofluids. The ineffectiveness of both single phase and two phase nanoparticles has led to increased demand for hybrid nanofluids as a salvaging remedial action. They display high rate of thermal conductivity but using small quantities of nanoparticles dispersed in base fluid.

In a study by Bahram & Akbari [6] using silver and copper oxide with equal ratio of 1:1 in water and ethylene glycol-based hybrid nanofluids at different volume fractions reported an improved thermal conductivity. Thus the present work embed much focus on investigating the performance of two nanoparticles (CuO and ZnO) in varying concentrations for better heat transfer agglomerated in ethylene glycol-water based fluid as a coolant for radiators in automotive.

The use of ethylene glycol-based nanofluids in automobile radiators has been studied by Mutuku [7]. It was discovered that the heat transfer properties of the ethylene glycol-based nanofluid containing copper oxide, Aluminium oxide, and titanium dioxide were superior to those of the convective fluids. Sundar [8] in their experiment tested three-dimensional laminar flow and heat transfer over the flat tubes of a car radiator using ethylene glycol and water as well as copper oxide and aluminum oxide as nanofluid base fluids. The convective heat transfer coefficient along the flat tubes was significantly boosted by the nanofluid flow in comparison to the base fluid. Under extremely turbulent flow conditions, the nanofluids demonstrated an impressive increase of 45% as compared to pure water. In a different study, Aluminium oxide nanoparticles and ethylene glycol were used to increase the cooling effectiveness of automobile radiators by Choi [1]. They realized that adding nanofluids to a car radiator greatly improves cooling performance.

In a study by Madhesh [8], they investigated on the effects of titanium oxide and Aluminium oxide nanoparticles on the thermal conductivity of water-based nanofluids. They noted that at 32oc, nanofluids containing water and 3.9 vol% alumina had a 30.6% improvement in effective thermal conductivity. The volume proportion at which thermal conductivity improved by 20% was determined to be 4% in experiments using copper oxide-water/ethylene glycol nanofluids and Aluminium oxide- water/ethylene glycol nanofluids Mehta [9].

It is also evident that water is the primary fluid used by researchers with nanoparticles predominantly composed of copper (II) oxide and Aluminium oxide. Water and ethylene glycol are often used as base fluids though not compared anywhere in the literature. As a result, a comparison of water and ethylene glycol as base fluids and provided guidance on which would be the most useful Nanofluid as a radiator coolant. The features of Nanofluid coolants with copper oxide, alumina, copper and zinc oxide nanoparticles were investigated in depth. Skin friction, the Reynolds number and the local Nusselt number of the underlying fluids were also studied along with their sensitivity to the nanoparticles' presence.

MATHEMATICAL FORMULATION

A two dimensional, steady and incompressible flow of an electrically charged ethylene glycol based hybrid nanofluid passed over a heated semi-infinite flat plate under influence of an induced magnetic field is considered. The strength of the magnetic field will be constant throughout the flow. The magnetic Reynolds number is small as there is no applied voltage. The induced magnetic field and wall effects are thus negligible. The surface on which the fluid flows stretches at a constant rate, U_0 with a temperature T_w. In a free stream, the wall is assumed to be stationary as the temperature is maximized to T_∞.

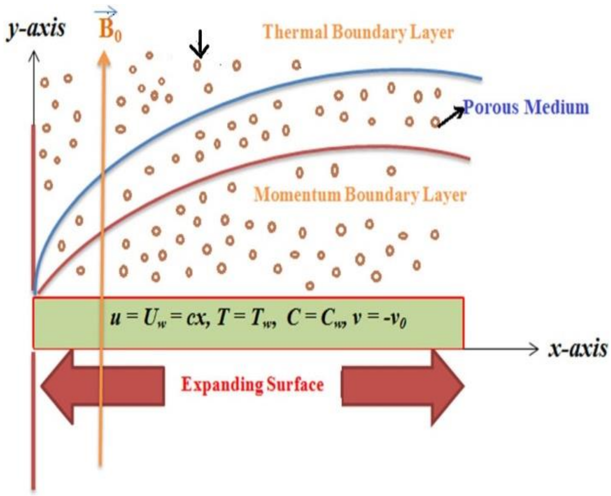

Fig. 1 Flow Configuration

Considering the hybrid nanofluid as a class of steam locomotive thermally at equilibrium and exhibiting stability between nanoparticles and the base fluid; under Boussinesq approximation, the equations governing the fluid flow are:

$$\frac{\partial u}{\partial x} + \frac{\partial u}{\partial y} = 0 \qquad (3.1.1),$$

$$u\frac{\partial u}{\partial x} + v\frac{\partial u}{\partial y} = \frac{\mu_{hnf}}{\rho_{hnf}}\frac{\partial^2 u}{\partial y^2} + g\beta_{hnf}(T - T_\infty) - \frac{\sigma_{hnf}}{\rho_{hnf}}B_0^2 u \dots\dots (3.1.2),$$

$$u\frac{\partial T}{\partial x} + v\frac{\partial T}{\partial y} = \frac{k_{hnf}}{(\rho C_p)_{hnf}}\frac{\partial^2 T}{\partial y^2} + \frac{\mu_{hnf}}{(\rho C_p)_{hnf}}\left(\frac{\partial u}{\partial y}\right)^2 + \frac{\sigma_{hnf} B_o^2 u^2}{(\rho C_p)_{hnf}}, \quad (3.1.3),$$

The boundary conditions at the surface of the plate and at the free stream are:

$$at\ y = 0; \quad u(x,0) = U_0, v(x,0) = 0$$

$$-k_f\frac{\partial T}{\partial y}(x,0) = h_f\left(T_f - T(x,0)\right)$$

$$as\ y \to \infty; u(x,\infty) = 0, T(x,\infty) = T_\infty \dots \ (3.1.3.2)$$

The quantities of practical interest are the coefficient of skin friction and Nusselt number given as:

$$C_f = \frac{\tau_w}{\rho_f u_w^2}, Nu = \frac{x q_w}{K_{hnf}}(T_w - T_\infty),$$

where, $\tau_w = \mu_{hnf}\frac{\partial u}{\partial y}\Big| y = 0, q_w = -K_{hnf}\frac{\partial T}{\partial y}\Big| y = 0.$

Assuming that the nanoparticles are well dispersed and uniformly distributed in the entire system, the effective thermo-physical properties of the hybrid nanofluid can be evaluated using equation (3.1.4). The very relations can be used to predict physical properties of the hybrid nanofluids, for instance, density, viscosity, thermal conductivity, specific heat capacity and volume fraction.

$$\begin{cases} \mu_{hnf} = \dfrac{\mu_f}{(1-\emptyset)^{2.5}}, \beta_{hnf} = (1-\emptyset)\beta_f + \emptyset\beta_n \\ \dfrac{k_{hnf}}{k_f} = \dfrac{(k_n + 2k_f) - 2\emptyset(k_f - k_n)}{(k_n + 2k_f) + \emptyset(k_f - k_n)}, (\rho C_p)_{hnf} = (1-\emptyset)(\rho C_p)_f + \emptyset(\rho C_p)_n \\ \sigma_{hnf} = \sigma_f\left[1 + \dfrac{2(r-1)\emptyset}{(r+2)-(r-1)\emptyset}\right], r = \dfrac{\sigma_n}{\sigma_f}, \rho_{hnf} = (1-\emptyset)\rho_f + \emptyset\rho_n, \alpha_{hnf} = \dfrac{k_{hnf}}{(\rho C_p)_{hnf}}, \\ \alpha_f = \dfrac{k_f}{(\rho C_p)_f}, \quad v_f = \dfrac{\alpha_f \mu_f C_p}{k_f} \end{cases} \quad \ldots (3.1.4)$$

Where $\emptyset$ is the nanoparticle volume fraction ($\emptyset$=0 relates to a regular fluid), ρ_f and ρ_n being densities of base fluid and nanoparticles respectively, $(\rho C_p)_{hnf}$ and $(\rho C_p)_n$ are the heat capacitance of nanofluid and nanoparticles respectively and σ_n and σ_f the electrical conductivity of the nanoparticles and the base fluid respectively.

The stream function ψ(x,y) defined as $u = \frac{\partial \psi}{\partial y}$ and $v = -\frac{\partial \psi}{\partial x}$ satisfies the continuity equation (3.1.1).

To simplify the mathematical analysis of the problem, the following similarity transformations are used:

$$\xi = \sqrt{\left(\frac{\alpha}{v_f}\right)}y, \psi = \sqrt{(\alpha v_f)}\, x f(\xi) \text{ and } \theta(\xi) = \frac{T - T_\infty}{T_w - T_\infty} \ldots\ldots\ldots\ldots\ldots\ldots\ldots 3.1.5$$

where ξ is the similarity variable, $f(\xi)$ is the non-dimensional stream function and $\theta(\xi)$ the non-dimensional temperature function. Introducing equation 3.1.5 into equations 3.1.2 and 3.1.3 respectively yields the following O.D.Es:

$$\begin{aligned} f''' &+ (1-\emptyset)^{2.5}\left(1-\emptyset+\emptyset\frac{\rho_n}{\rho_f}\right)ff'' - (1-\emptyset)^{2.5}\left(1-\emptyset+\emptyset\frac{\rho_n}{\rho_f}\right)(f')^2 \\ &- Ha(1-\emptyset)^{2.5}\left(1-\emptyset+\emptyset\frac{\sigma_n}{\sigma_f}\right)f' \\ &+ Gr(1-\emptyset)^{2.5}\left(1-\emptyset+\emptyset\frac{\beta_n}{\beta_f}\right)\left(1-\emptyset+\emptyset\frac{\rho_n}{\rho_f}\right)\theta = 0 \ldots. \quad (3.1.6) \end{aligned}$$

$$\begin{aligned} \theta'' &+ \frac{k_f}{k_{hnf}}Pr\left(1-\emptyset+\emptyset(\rho C_p)_n/(\rho C_p)_f f\theta' + \frac{k_f EcPr}{k_{hnf}(1-\emptyset)^{2.5}}(f'')^2\right) \\ &+ \frac{k_f HaEcPr}{k_{hnf}}\left(1-\emptyset+\emptyset\frac{\sigma_n}{\sigma_f}\right)(f')^2 = 0 \quad (3.1.7) \end{aligned}$$

Subject to the boundary conditions;

$$f(0) = 0, f'(0) = 1, \theta'(0) = Bi[\theta(0) - 1], f'(\infty) = 0, \theta'(\infty) = 0 \ldots\ldots\ldots\ldots (3.1.8)$$

Where the primes denotes differentiation w.r.t η and the Harmatan number Ha, Grashof number Gr, Prandtl number Pr, Eckert number Ec and Biot number Bi can be obtained as follows:

$$Ha = \frac{\sigma_f B_0^2 x}{\rho_f U_0}, Gr = \frac{\beta_f g(T_f - T_\infty)}{U_0 a}, Ec = \frac{U_0^2}{(\rho C_p)_f (T_f - T_\infty)}, Bi = \frac{h_f}{k_f}\sqrt{\frac{v_f x}{U_0}}, Pr = \frac{v_f}{\alpha_f} \ldots 3.1.9)$$

The physical quantities of practical significance are skin friction coefficient Cf and the Nusselt number Nu which are defined as: $C_f = \frac{\tau_w}{\rho_f U_0^2}$,

$$Nu = \frac{x q_w}{k_f(T_f - T_\infty)} \ldots\ldots\ldots\ldots\ldots\ldots\ldots\ldots (3.1.10)$$

Where τ_w is the skin friction and q_w is the heat flux from the plate and can be determined as follows: $\tau_w = \mu_{hnf}\frac{\partial u}{\partial y}|y = 0, q_w = -k_f\frac{\partial T}{\partial y}|y = 0 \ldots\ldots\ldots\ldots\ldots\ldots\ldots\ldots\ldots.. (3.1.11)$

Putting equation (3.1.27) into (3.1.26), we get;

$$C_{f_x} = Re^{\frac{1}{2}} C_f = \frac{1}{(1-\emptyset_1)^{2.5}(1-\emptyset_2)^{2.5}} f''(0),$$

$$Nu_x = Re^{-\frac{1}{2}} Nu = -\frac{k_{hnf}}{k_f}\theta'(0) \ldots\ldots\ldots\ldots (3.1.12)$$

Where C_{f_x} and Nu_x are the local skin friction and local Nusselt number respectively and the Reynolds number given as follows: $Re = \frac{U_0 x}{v_f}$.

NUMERICAL PROCEDURE

The set of equations (3.1.6) – (3.1.7) under the boundary conditions (3.1.8) is a coupled nonlinear boundary valued problem that can be solved numerically using the shooting technique with Runge-Kutta-Felhberg integration scheme. This method transforms the equation into a set of initial value problems containing unknown initial values which are to be determined by guessing. The fourth-order Runge-Kutta-Felhberg iteration method is applied to integrate the set of initial value problems until the given boundary conditions are satisfied. Defining the new variables as:

$x_1 = f, x_2 = f', x_3 = f'', x_4 = \theta, and\ x_5 = \theta'$ (3.1.13), reduces equations (3.1.6) – (3.1.7) to systems of first order differential equations:

$$x_3' = Ha\left[1 + \frac{3(r-1)\varphi}{(r+2)-(r-1)\varphi}\right](1-\emptyset)^{2.5}x_2 - (1-\emptyset)^{2.5}\left(1-\emptyset+\emptyset\frac{\rho_n}{\rho_{hnf}}\right)x_1 x_3$$
$$- Gr(1-\emptyset)^{2.5}\left(1-\emptyset+\emptyset\frac{\beta_n}{\beta_{hnf}}\right)\left(1-\emptyset+\emptyset\frac{\rho_n}{\rho_{hnf}}\right)x_4$$
$$+ (1-\emptyset)^{2.5}\left(1-\emptyset+\emptyset\frac{\rho_n}{\rho_{hnf}}\right)x_2^2 \quad (3.1.14)$$

$$x_5' = -\frac{k_f}{k_{hnf}}Pr\left(1-\emptyset+\emptyset\frac{(\rho C_p)_n}{(\rho C_p)_{hnf}}\right)x_1 x_5 - \frac{k_f Ec Pr}{k_{hnf}(1-\emptyset)^{2.5}}x_3^2$$
$$-\left[1 - \frac{3(r-1)\varphi}{(r+2)-(r-1)\varphi}\right]\frac{k_f Ha Ec Pr}{k_{hnf}}x_2^2 \quad (3.1.15)$$

Subject to the initial conditions:

$$x_1(0) = 0, x_2(0) = 1, x_5(0) = Bi[x_4(0) - 1], x_2(0) = s_1, x_5(0) = s_2 \quad (3.1.16)$$

In the shooting process, s_1 and s_2 in Eq. (3.1.16) are assumed and Eqs. (3.1.14) – (3.1.15) integrated numerically as an initial valued problem to a given terminal point. The assumed missing initial conditions' accuracy was checked by comparing the calculated value of the dependent variable at the terminal point with its given value there. Improved values of the missing initial conditions are obtained in case of any differences. The entire computation procedure is implemented using MATLAB. The boundary valued problems are automatically solved by the dsolve command as long as the appropriate algorithm is applied.

The present method is unconditionally stable and has been successfully used by Mutuku *et al.*,[10] to solve various problems in fluid mechanics and heat transfer. From the process of numerical computation, the fluid velocity, temperature, skin friction coefficient and local Nusselt number are presented by $f'(\eta), \theta(\eta), f''(\eta) and\ \theta'(\eta)$ respectively.

RESULTS AND DISCUSSION

We consider (Cu-Al2O3), (Cu-ZnO) and (CuO-ZnO) as the hybrid nanoparticle combination for use to prepare the hybrid nano-coolant. The hybrid nanoparticle combinations are then suspended in Ethylene-glycol base fluid. The graphical illustration of the results is given in Figs. (3.1 – 4.6). The conclusion drawn from the flow is crucial while determining the optimal hybrid nanoparticle combination for the hybrid nano-coolant for industrial applications. Ha = 0 denotes absentia of magnetic field and ϕ1 = ϕ2 =0 represents the regular fluid. The thermal physical properties of Ethylene Glycol and the nanoparticles are shown the table 1 below:

Table 1: Ethylene Glycol, Water, and Nanoparticles, and Their Thermophysical Characteristics

Material	Density $\rho(kgm^{-3})$	Heat capacity $C_p(J/Kgk)$	Thermal conductivity K(w/mk)	B x$10^{-5}(K^{-1})$	σ(s/m)	Viscosity $\mu(Nm^{-2})$
Copper	8933	385	401	1.67	$5.95x10^6$	-
Silver	10500	235	429	1.89	$6.3x10^7$	-
Aluminium	2701	902	237	2.31	$3.5x10^7$	-
Copper oxide	6510	540	18	0.85	$5.96x10^7$	-
Alumina	3970	765	40	0.85	$3.5x10^6$	-
Zinc oxide	4250	686.2	8.9538	0.9	$2.38x10^6$	-
Ethylene glycol	1114	2415	0.252	57	$1.07x10^{-6}$	0.00304
Pure water	997.1	4179	0.613	21	$5.5x10^{-6}$	-
Engine oil	884	1909	0.145	70	$1.0x10^{-7}$	-

Dimensionless Velocity and Temperature profiles of Cu-Al2O3, Cu-ZnO and CuO-ZnO Ethylene Glycol-water based Hybrid Nanocoolants:

\

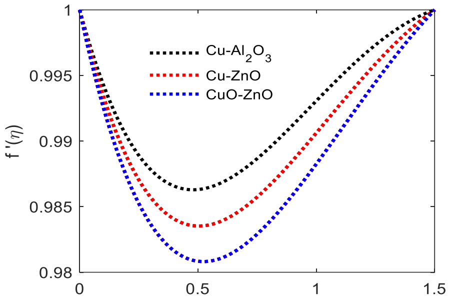

Fig. 3.1 Dimensionless velocity nanofluids

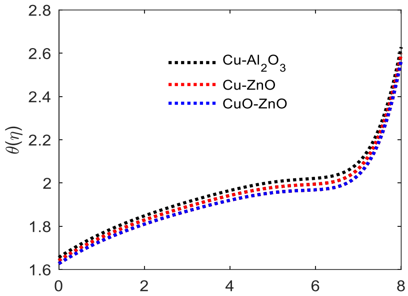

Fig. 3.2 Temperature profile of nanofluids

$\boldsymbol{Pr = 0.5, Ha = 0.2, Ec = 0.1, Gr = 0.1, \beta = 0.2, \phi = 0.03}$. $\boldsymbol{Pr = 0.5, Ha = 0.2, Ec = 0.1, Gr = 0.1, \beta = 0.2, \phi = 0.014}$

Figures 3.1 and 3.2 give the primary velocity profiles and temperature profiles of ethylene-glycol based ((Cu-Al2O3), (Cu-ZnO), and (CuO-ZnO) hybrid nano-coolants. From the fig. 3.1, the momentum boundary thickness of Cu-ZnO/EG hybrid nano-coolant is thinner compared to that of other hybrid nano-coolant. This is attributed to the fact that Cu-ZnO hybrid nanoparticles combination is highly susceptible to effects of magnetic field. For Fig.3.2, both hybrid nano-coolants exhibit highest temperature close to the surface of the plate which decays to zero away from the surface of the plate. This then satisfies the given free stream condition.

Dimensionless Velocity and Temperature Profiles of (Cu-Al_2O_3), (Cu-ZnO) and (CuO-ZnO)/EG hybrid nano-coolant:

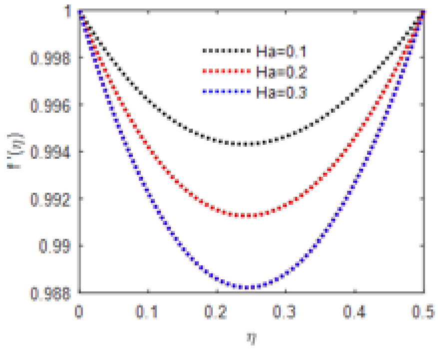

Pr=2.5,Ha=0.3,Ec=0.2,Gr=0.1,β=0.2,ϕ=0.5.

Fig. 3.3 Effects of Ha on primary velocity

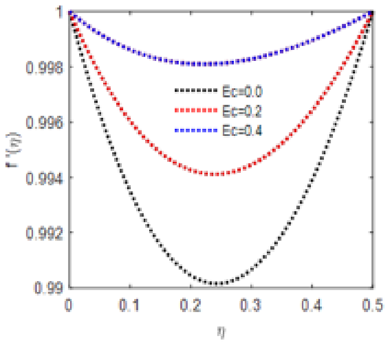

Fig. 3.6 Effect of Eckert number on primary velocity.

Pr=2.5,Ha=0.1,Ec=0.4,Gr=0.1,β=0.2,ϕ=0.5

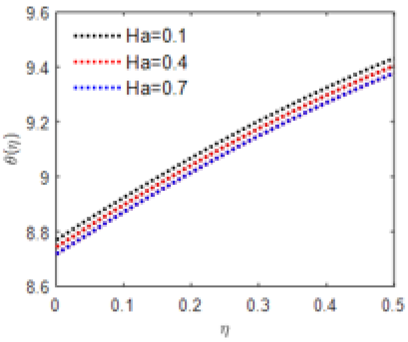

Pr=2.5,Ha=0.7,Ec=0.2,Gr=0.1,β=0.2,ϕ=0.5

Fig. 3.4 Effect of Ha on temperature profile.

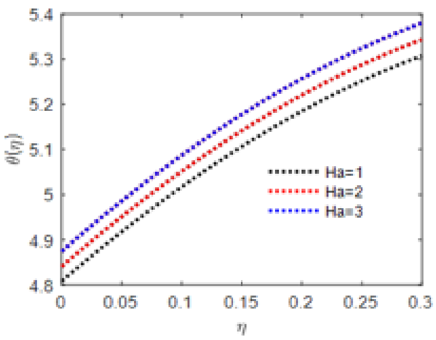

Fig. 3.7 Effect of Ha on temperature profile.

Pr=3.5,Ec=1.2,Gr=0.5,β=0.6,ϕ=0.5

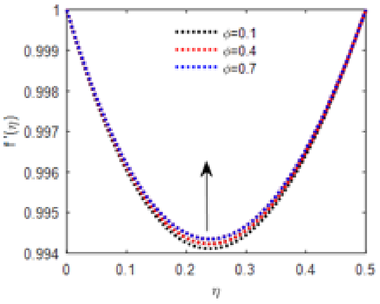

Fig. 3.5 Effects of volume fraction on velocity profile.

Pr=2.5,Ha=0.1,Ec=0.2,Gr=0.1,β=0.2,ϕ=0.5

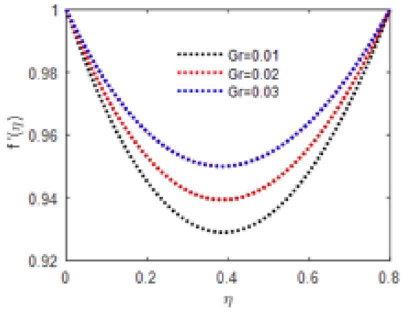

Fig. 3.8 Effect of Grashof number on primary velocity.

Pr=3.5,Ha=0.1,Ec=1.2,Gr=0.03,β=0.6,ϕ=0.5

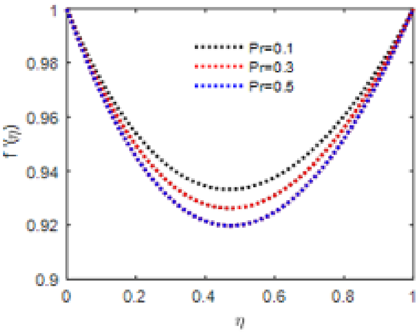

Fig. 3.9 Effect of Prandtl number on primary velocity.

Ha=0.1,Ec=1.2,Gr=0.1,β=0.6,ϕ=0.5

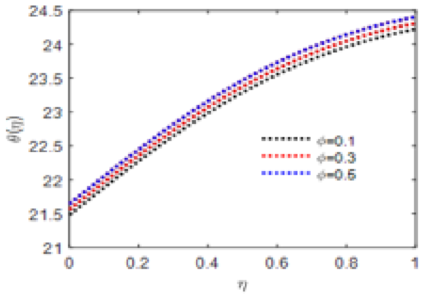

Fig. 4.0 Effect of volume fraction on primary velocity.

Pr=2.5,Ha=0.1,Ec=0.2,Gr=0.1, β=0.2.

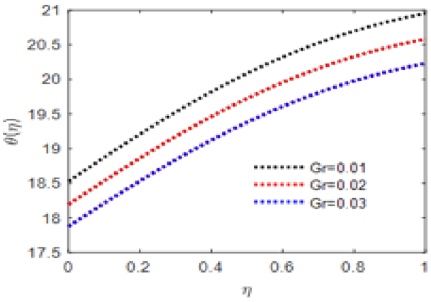

Fig. 4.1 Effect of Grashof number on temperature.

Pr=2.5,Ha=0.1,Ec=0.2,β=0.2,ϕ=0.5

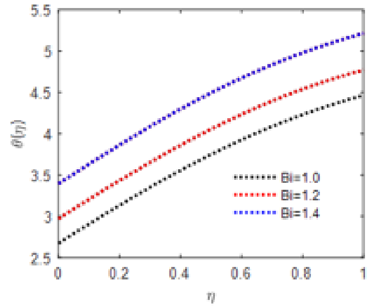

Fig. 4.2 Effect of Biot number on velocity profile.

Pr=1.5;Ha=0.3,Ec=0.2,Gr=0.5,ϕ=0.5

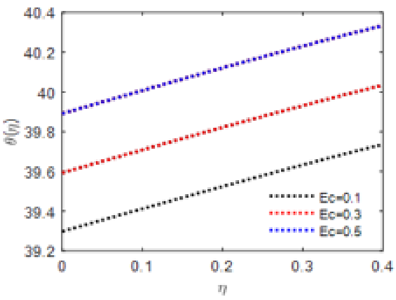

Fig.4.3 Effect of Eckert number on primary temperature profile.

Pr=1.5,Ha=0.3,Gr=0.5,β=0.03,ϕ=0.5

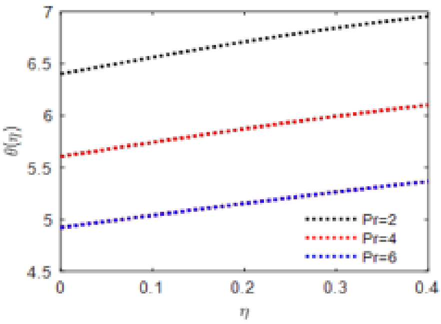

Fig.4.4 Effect of prandtl number on temperature
Ha=0.3,Ec=0.03,Gr=0.5,β=0.3,ϕ=0.5

Figs.3.3 and 3.4 illustrates the effects of magnetic intensity (Ha) on primary velocity profiles of the three hybrid nano-coolants. Primary velocity of the hybrid nano-coolant decreases with increasing values of Ha (Ha =0.1, 0.2, 0.3). Magnetic field present in the flow generates the Lorentz force. This is attributed to the motion of conducting fluid in the presence of a magnetic field retards the flow of the fluid.

Figs. 3.5 and 3.6 illustrate the effect of nanoparticle volume fraction and Eckert number on primary velocity profiles of the three hybrid nano-coolants under study. From Fig.3.5, the primary velocity profiles of the nano-coolant increases with increase in the volume fraction (ϕ) of the nanoparticle (ϕ=0.1, 0.4, 0.7). In Fig. 3.6, the primary velocity profile of the three hybrid nanofluids increases with increase in the Eckert number (Ec=0.0, 0.2, 0.4).

Fig. 3.7 shows temperature profiles of the three-hybrid nano-coolants with increase in Ha (Ha =0.1, 0.4, 0.7). From the figure, the temperature of the nanofluid increases with increase in values of Ha. The induced magnetic field causes heat generation. This is caused by increase in force of friction between the layers of the fluid which generate heat that increases the temperature of hybrid nanofluid.
Fig. 3.8 shows the effect of increasing Grashof number on primary velocity profiles of the hybrid nano-coolants. From the figure, primary velocity profiles of the hybrid nano-coolant increases with increase in the Grashof number (Gr=0.01, 0.02, 0.03)
Fig. 3.9 shows the effect of Prandtl number on primary velocity profiles of Cu-Al_2O_3, Cu-ZnO and CuO-ZnO)/EG hybrid nano-coolant. From the figure, velocity profiles decreases with increase in the values of the Prandtl number (Pr=0.1, 0.2, 0.3)

Figs (4.0- 4.4) shows the effect of volume fraction, Grashof number, Biot number, Eckert number and Prandtl number on temperature profiles ,$\Theta(\eta)$, of the three hybrid nano-coolants. Fig. 4.0 is plotted for increasing values of nanoparticle volume fraction (ϕ=0.1, 0.4, 0.7), fig. 13 is plotted for increasing values of Grashof number (Gr =0.01, 0.02, 0.03). The results show that the temperature profile of the nano-coolant increases with increase in nanoparticle volume fraction and decreases with increase in Grashof number. For fig. 4.2- 4.3), the temperature profiles for the hybrid nano-coolant is plotted for increasing values of Biot number (Bi =1.0, 1.2, 1.4) and Eckert number (Ec = 0.1, 0.3, 0.5) respectively. In both, the temperature profiles increases with increase in values of Biot and Eckert numbers. Fig. 4.4 show the temperature profiles at different values of Prandtl number (Pr = 2.0, 4.0, 6.0). The temperature profiles of hybrid nano-coolant decreases with increase in values of Prandtl number.

Skin Friction Profiles and Nusselt Number Profiles of the Hybrid Nano-coolant (Cu-Al_2O_3), (Cu-ZnO) and (CuO-ZnO)/ EG:

Figs. 4.5 and 4.6 shows the Skin friction profiles and Nusselt number profiles of the hybrid nano-coolants at the surface of the plate. The skin friction coefficient and the local Nusselt number decreases with increase in the nanoparticle volume fraction (ϕ). CuO-ZnO/EG hybrid nanofluid is preferable as it moves closer to the surface of the plate thus elevating the velocity gradient at the plate surface. This then increases the skin friction at the plate surface. From the engineering and industrial application point of view, CuO-ZnO/EG hybrid nanofluid would be the best coolant owing to these features.

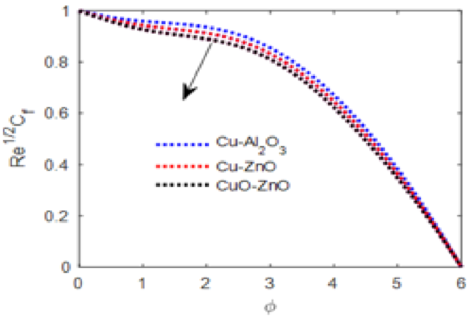

Fig. 4.5 Effect of volume fraction on Skin friction

Pr=4.8,Ha=0.2,Ec=0.3,Gr=1.2,β=0.2

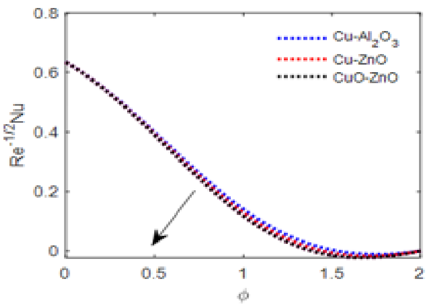

Fig. 4.6 Effect of volume fraction on Nusselt number

Pr=4.5,Ha=0.2,Ec=0.1,Gr=1.1,β=0.2

CONCLUSION

Three different ethylene-glycol based hybrid nano-coolants, that is, Cu- Al_2O_3, Cu- ZnO and CuO- ZnO have been numerically investigated to determine the best coolant for use in a car radiator. The performance of Cu- ZnO and CuO- ZnO with varying concentration as a better heat transfer hybrid nanofluid in comparison to convective fluids such as water was investigated using numerical approaches. The following conclusions can be drawn from this study:

- The hybrid nanofluids exhibited better thermal conductivity than the mono nanofluids as well as water. For instance, a better enhanced thermal conductivity was observed for Cu- ZnO and a superior one with CuO- ZnO. More so, thermal conductivity of hybrid nanofluids significantly increased with the increasing volume concentration of the hybrid nanoparticles suspended in the base fluid. In respect to this, Cu- ZnO/EG hybrid nanofluid with 0.5% volume concentration exhibited higher thermal conductivity.

- A higher viscosity was observed for the hybrid nanofluids than for base fluids. It increases with increase in volume concentration of nanoparticles. Cu- ZnO and CuO- ZnO/EG-water exhibited higher viscosity compared to base fluids. High viscosity results from great friction between the nanoparticles in momentum.

- The velocity of the hybrid nanofluids decreases with increase in values of magnetic field strength, Prandtl number. It however, increased with increase in Eckert number, Grashof number and volume fraction. As nanoparticles collide the magnetic field is induced with great heat liberation.

- The temperature of the hybrid nanofluids increases with increase in magnetic field strength, Biot number, Eckert number and nanoparticle volume fraction. It however decreases with increase in Grashof number and Prandtl number. Temperature rise result from heat energy produced due to friction between reacting nanoparticles as well as their increased kinetic energy.

- For all the three hybrid nanofluids, the skin friction and local Nusselt number decreases with increase in the volume fraction of the nanoparticles. The increase in volume fraction increases the concentration of the reacting particles as well as the friction force. This reduces the kinetic energy of the nanoparticles as well as rate of heat liberation.

RECOMMENDATIONS

Automotive industries are working towards customer satisfaction during aerodynamics designing. Efficiency of the devices depends much on the type of coolant used. Based on the outcomes of this study, the following recommendations are made:

- To increase the heat transfer rates, Cu- ZnO/EG-water hybrid nanofluid should be considered over convectional fluids used.
- To reduce the skin friction in the flow with thermal radiation, Cu- ZnO/EG-water hybrid nanofluid should be considered over the convectional fluids e.g water.
- To increase the rate of heat transfer of the Cu- ZnO/EG-water hybrid nanofluid, the nanoparticles should be well sonicated.
- The fluid flow velocity can be curbed by varying the volume fraction of the hybrid nanofluid.

REFERENCES

1. Afrand, M. Toghraie, D. Ruhani, B (2019). Effects of temperature and nanoparticles concentration on rheological behavior of Fe3O4- Ag/EG hybrid nanofluids: An experiment study. Exp. Therm. Fluid Sci., 77, 38-44.
2. Bahrain, M. Akbari, M. Karipour, Afrand, M. An experimental study on rheological behavior of hybrid nanofluids made of iron and copper oxide in a binary mixture of water and ethylene glycol: Non-Newtonian behavior. Exp. Therm. Sci. 2022, 79, 231-237.
3. Cakmak, N. K., Said, Z., Sundar, L. S., Ali, Z. M., & Tiwari, A. K. (2020). Preparation, characterization, stability, and thermal conductivity of rGO-Fe3O4-TiO2 hybrid nanofluid: An experimental study, Powder technology, 372, 235-245.
4. Choi SUS, Yu .W, Hull J.R, Zhang Z.G, Lockwood F.E. (2018), Nanofluids for vehicle thermal management, Society of Automotive Engineers; p 139- 144.
5. Dhaiban, H.T. Delavari, (2016). Numerical Study of heat transfer enhancement in heat exchanger using Al2O3 nanofluids. J Eng., 22, 98-115.
6. Hussein A.M. Leong (2021), Thermal performance and thermal properties of hybrid nanofluids laminar flow in a double pipe heat exchanger. Experimental thermal and Fluid Science; 88:52-59.
7. Kimulu, A. M., Mutuku.W. N., & Mutua, N. M. (2018). Car Antifreeze and Coolant: Comparing Water and Ethylene Glycol as Nano Fluid Base Fluid. International Journal of Advances in Scientific Research and Engineering, 4(6), 17-37.
8. L.Sundar, Md.H. Farooky, S.N. Sarada, M.K. Singh (2020). Experimental thermal conductivity of ethylene glycol and water based, low volume concentration of Aluminium oxide and CuO nanofluids, Int Comm Heat mas transf. p 41-46.
9. Madhesh, D, Parameshwaran. R,Kalaiselvam, S. (2019), Experimental investigation on convective heat transfer and rheological characteristics of Cu- TiO2 hybrid nanofluids. Experimental Thermal and Fluid science; 52: 104-115.
10. Makinde O.D, Mutuku W.N (2014) Hydro magnetic thermal boundary layer of nanofluids over a convectively heated flat plate with viscous dissipation and ohmic heating. UPB Sci Bull Ser A 76(2):181–192.
11. Mehta, B., Subhedar, D., Panchal, H., & Said, Z. (2019). Synthesis, stability, thermophysical properties and heat transfer applications of nanofluid–a review. *Journal on Molecular Liquids*, 120034.
12. Mutuku, W. N., Makinde OD (2014) on hydro magnetic boundary layer flow of nanofluids over a permeable moving surface with Newtonian heating. Lat Am Appl Res 44(1):57–62
13. Mutuku, W. N. (2016). Ethylene glycol (EG)-based nanofluids as a coolant for automotive radiator. *Asia* Pacific Journal on Computational Engineering, 3, 1-15.
14. Mutuku-Njane, Makinde. OD (2014) MHD nanofluid flow over a permeable vertical plate with convective heating. J Computational and Theoretical Nanoscience 11(3): 667-675.
15. Raei B, Shahraki F, Jamialahmadi M, Peyghambarzadeh SM (2019), Experimental study on heat transfer and flow properties of Y-Al_2O_3/Water nanofluids in a double-tube heat exchanger. Journal of Thermal analysis and Calorimetry; 127(3): 2561-2575.
16. Yan S.R, Toghraie D, abdulkareem LA, Alizedeh A, Barnoon P, Afrand M. (2020), Rheological behavior of MWCNTs- ZnO/Water-Ethylene glycol hybrid non- Newtonian nanofluids by use of an experimental investigation. Journal of Materials Research and Technology, 9(4):8401-8406